

Vegetation response to extreme climate events on the Mongolian Plateau from 2000 to 2010

This content has been downloaded from IOPscience. Please scroll down to see the full text.

2013 Environ. Res. Lett. 8 035033

(<http://iopscience.iop.org/1748-9326/8/3/035033>)

View [the table of contents for this issue](#), or go to the [journal homepage](#) for more

Download details:

IP Address: 103.9.90.228

This content was downloaded on 30/03/2014 at 11:39

Please note that [terms and conditions apply](#).

Vegetation response to extreme climate events on the Mongolian Plateau from 2000 to 2010

Ranjeet John¹, Jiquan Chen^{1,2}, Zu-Tao Ou-Yang¹, Jingfeng Xiao³,
Richard Becker¹, Arindam Samanta⁴, Sangram Ganguly⁵,
Wenping Yuan⁶ and Ochirbat Batkhishig⁷

¹ Department of Environmental Sciences, University of Toledo, Toledo, OH 43606, USA

² Institute of Botany, Chinese Academy of Sciences, No. 20 Nanxincun, Xiangshan, Beijing 100093, People's Republic of China

³ Earth Systems Research Center, Institute for the Study of Earth, Oceans, and Space, University of New Hampshire, Durham, NH, USA

⁴ Atmospheric and Environmental Research Incorporated, Boston, MA, USA

⁵ Bay Area Environmental Research Institute and NASA Ames Research Center, Moffett Field, CA 94035, USA

⁶ College of Global Change and Earth System Science, Beijing Normal University, Beijing 100875, People's Republic of China

⁷ Institute of Geography, Mongolian Academy of Sciences, Ulaanbaatar, 210620, Mongolia

E-mail: ranjeet.john@utoledo.edu

Received 7 February 2013

Accepted for publication 13 August 2013

Published 29 August 2013

Online at stacks.iop.org/ERL/8/035033

Abstract


Climate change has led to more frequent extreme winters (aka, *dzud*) and summer droughts on the Mongolian Plateau during the last decade. Among these events, the 2000–2002 combined summer drought–*dzud* and 2010 *dzud* were the most severe on vegetation. We examined the vegetation response to these extremes through the past decade across the Mongolian Plateau as compared to decadal means. We first assessed the severity and extent of drought using the Tropical Rainfall Measuring Mission (TRMM) precipitation data and the Palmer drought severity index (PDSI). We then examined the effects of drought by mapping anomalies in vegetation indices (EVI, EVI2) and land surface temperature derived from MODIS and AVHRR for the period of 2000–2010. We found that the standardized anomalies of vegetation indices exhibited positively skewed frequency distributions in dry years, which were more common for the desert biome than for grasslands. For the desert biome, the dry years (2000–2001, 2005 and 2009) were characterized by negative anomalies with peak values between -1.5 and -0.5 and were statistically different ($P < 0.001$) from relatively wet years (2003, 2004 and 2007). Conversely, the frequency distributions of the dry years were not statistically different ($p < 0.001$) from those of the relatively wet years for the grassland biome, showing that they were less responsive to drought and more resilient than the desert biome. We found that the desert biome is more vulnerable to drought than the grassland biome. Spatially averaged EVI was strongly correlated with the proportion of land area affected by drought ($PDSI < -1$) in Inner Mongolia (IM) and Outer Mongolia (OM), showing that droughts substantially reduced vegetation activity. The correlation was stronger for the desert biome ($R^2 = 65$ and 60 , $p < 0.05$) than for the IM grassland biome ($R^2 = 53$,



Content from this work may be used under the terms of the [Creative Commons Attribution 3.0 licence](http://creativecommons.org/licenses/by/3.0/). Any further distribution of this work must maintain attribution to the author(s) and the title of the work, journal citation and DOI.

$p < 0.05$). Our results showed significant differences in the responses to extreme climatic events (summer drought and *dzud*) between the desert and grassland biomes on the Plateau.

Keywords: Mongolian Plateau, vegetation indices, extreme climate, drought, land surface temperature, MODIS, EVI, EVI2, *dzud*

 Online supplementary data available from stacks.iop.org/ERL/8/035033/mmedia

1. Introduction

Over the past century, extreme climate events (e.g., drought, extreme temperatures) have increased in frequency and severity globally, particularly in central and northern Eurasia (Groisman *et al* 2009, Hansen *et al* 2010). The major drought events during the last decade include the prolonged 2000–2004 drought in western North America (Schwalm *et al* 2012), the 2003 summer heat wave in Europe (Teuling *et al* 2010), the Amazon basin droughts of 2005 and 2010 (Lewis *et al* 2011, Philips *et al* 2009), the widespread, severe drought from 2001 to 2007 in Australia (Ponce-Campos *et al* 2013), the severe drought in China in 2010 (Zhang *et al* 2012) and the sustained drought on the Mongolian Plateau from 1999 to 2002 (Fernández-Giménez *et al* 2012).

The Mongolian Plateau has experienced several extreme climate events during the past decade, including extreme winters (referred to as *dzuds* in Mongolia) and summer droughts, sometimes both in the same year (drought–*dzud* combinations). The frequency and amplitude of these extreme events has increased in the 2000–2010 period compared to the few decades prior to 2000 (supplementary table 1, supplementary figures 4 and 5 available at stacks.iop.org/ERL/8/035033/mmedia). The most important events were perhaps the combined summer drought–*dzud* events of 2000–2002 and the *dzud* of 2010 (Angerer *et al* 2008, Fernández-Giménez *et al* 2012, supplementary table 1 available at stacks.iop.org/ERL/8/035033/mmedia). Droughts on the Mongolian Plateau are characterized by precipitation and soil moisture deficits with Palmer drought severity index (PDSI) values > -2 to > -5 (Davi *et al* 2010). *Dzuds* typically feature extreme cold, heavy snowfall, reduced availability of forage and widespread mortality of livestock (Tachiiri *et al* 2008, Morinaga *et al* 2003). When a *dzud* is preceded by a summer drought, the combined summer drought–*dzud* often leads to even higher mortality of livestock (Fernández-Giménez *et al* 2012). The consecutive 1999–2002 summer drought–*dzud* was the worst of the last 50 years when 30% of the national herd perished (Fernández-Giménez *et al* 2012, Tachiiri *et al* 2008). The 2009–2010 winter *dzud* was also very severe when 8.5 million livestock, 20% of the national herd, died during this period (Fernández-Giménez *et al* 2012). The warming and drying trends in Inner Mongolia were more significant during the last 30 years than in the preceding 20 years (Lu *et al* 2009). Previous studies also suggested that the five-year *dzud* cycles are related to the El Niño Southern Oscillation (ENSO) while the decadal cycles are influenced by the Indian monsoon (Morinaga *et al* 2003). Precipitation variability in the region is a function of

various forcings such as the westerly jet stream migrating northwards in summer, the Siberian anticyclone in winter, evapotranspiration and the monsoon (Aizen *et al* 2001, Iwao and Takahashi 2006). Extreme events like summer droughts and winter *dzuds* are expected to increase in frequency and magnitude (Fernández-Giménez *et al* 2012).

Ecosystem responses to these extreme climate events vary by biome on the Mongolian Plateau owing to differences in vegetation cover, precipitation, evapotranspiration and albedo (Donohue *et al* 2009, Snyder *et al* 2004, Yi *et al* 2010). Climate anomalies often show strong spatiotemporal variations (New *et al* 2000), indicating that any impact assessment should be site-specific (Qi *et al* 2012). To date, little research has examined the response of vegetation to *dzud* and combined summer drought–*dzud* for different biomes on the plateau using long-term satellite observations (Tachiiri *et al* 2008, Xu *et al* 2012).

Satellite-derived vegetation indices including the normalized difference vegetation index (NDVI) and the enhanced vegetation index (EVI) have been widely used as surrogates of vegetation canopy greenness and primary productivity (Myneni *et al* 1995, Huete *et al* 2006). Most vegetation greenness anomaly studies have focused on the effects of summer drought on forest biomes with significant carbon sequestration potential like the Amazon basin (Samanta *et al* 2010, Brando *et al* 2010, Lewis *et al* 2011, Xu *et al* 2011). The effects of extreme climate events in semiarid biomes, which cover 40–50% of the terrestrial surface and are home to 40% of the world population, have received relatively less attention (Reynolds *et al* 2007). There are few studies that focus on vegetation anomalies in semiarid regions (e.g., Xu *et al* 2012). Even fewer studies focus on the impacts of extreme winters unique to the Mongolian Plateau (Tachiiri *et al* 2008). In contrast with previous research based on vegetation greenness in the region that utilized the NDVI (Xu *et al* 2012), we made use of the EVI and EVI2 vegetation indices. Huete *et al* (2002) suggested that the use of NDVI in semiarid regions was questionable owing to its sensitivity to the soil background signature in areas with $< 50\%$ fractional cover. Consequently, EVI was proposed as it was not as sensitive to bright soil signatures and atmospheric effects.

Here we examined the responses of vegetation to extreme climate events on the plateau using the satellite-derived vegetation indices and land surface temperature. We identified the spatiotemporal dynamics in the anomalies of vegetation greenness using long-term earth observation records and examined the climate drivers of these anomalies using meteorological trends. Our specific questions are: (1) how does vegetation respond to climate extremes, throughout the

last decade across the Mongolian Plateau? and (2) were there any significant differences in the vegetation response among the biomes, or between the two political units, Inner and Outer Mongolia, especially during the extreme summer drought of 2001 and winter *dzud* of 2010?

2. Methods

2.1. Satellite data

We used monthly composites of EVI (MOD13A3), land surface temperature (LST, MOD11A2) and shortwave white sky albedo (MCD 43B3) (Collection 5) derived from the Moderate Resolution Imaging Spectroradiometer (MODIS) aboard the Terra satellite from 2000–2010. These datasets with a spatial resolution of 1 km represent a range of biophysical variables to identify anomalies during the past decade (figure 2).

While EVI anomalies can be obtained for the period 2000–2010 based on the decadal mean, they cannot be calculated for an earlier period as previous synoptic sensors (e.g., AVHRR) lacked a blue band that is needed for atmospheric correction (Jiang *et al* 2008). To complement the MODIS EVI, we used the new vegetation index and phenology (VIP) dataset of the NASA MEaSUREs (Making Earth System Data Records for Use in Research Environments) program (http://vip.arizona.edu/viplab_data_explorer.php#) (Jiang *et al* 2008). The VIP dataset consists of three decades (1981–2010) of consistent vegetation indices derived from AVHRR and MODIS and has a climate modeling grid (CMG) resolution of 5.6 km (0.05°). This new dataset enabled us to compute EVI2 anomalies in the past decade as deviations from a 30-year mean (1981–2010).

For the MODIS products, we only used the pixels with the highest quality in our analysis, through the use of standard quality control (QC bits) and LDOPE tools (https://lpdaac.usgs.gov/tools/ldope_tools) (Samanta *et al* 2012). EVI and EVI2 were used to examine the effects of summer droughts on vegetation greenness whereas the LST product was used to assess the effects of extreme winters. Shortwave white sky albedo was filtered with pixel reliability flag = 0 in the MCD43B2 product, to retain only the pixels that had undergone full BRDF inversion and was used to validate the EVI and EVI2 anomalies to account for false positives from clouds or contaminated pixels.

2.2. Climate data

We identified temperature and precipitation anomalies following Aragao *et al* (2007) and Anderson *et al* (2010). Previous studies have used merged Tropical Rainfall Measuring Mission (TRMM) data (Huffman *et al* 1995) to interpret vegetation index anomalies when the existing climate station network was sparsely distributed. We used the monthly precipitation rate (3B43 version 7, <http://disc.sci.gsfc.nasa.gov/>) to characterize precipitation deficits (Aragao *et al* 2007, Anderson *et al* 2010). Our study area is at the northern edge of TRMM coverage (50°N) and includes

the dominant land cover types of grassland and desert biomes in IM and OM. We also used the PDSI (Palmer 1965) to characterize drought severity and extent. PDSI, a widely used drought index (Dai *et al* 2004), is a measure of soil moisture that is currently available as compared to the long-term mean, and incorporates rainfall, soil moisture demand and supply (Palmer 1965). We obtained PDSI data at 0.5° × 0.5° resolution from the Numerical Terradynamic Simulation Group at the University of Montana (Zhao and Running 2010). The PDSI values range from –10 (dry) to –10 (wet). Mild drought is represented by values of –1 to –1.9, moderate drought by –2 to –2.9 and severe drought by <–3 (figure 3).

2.3. Analyses

We calculated standardized anomalies (sa) of satellite-based data as

$$sa = \frac{x - \bar{x}}{\sigma} \quad (1)$$

where sa is the standardized anomaly of a biophysical variable (e.g., vegetation greenness, LST, etc) for the dry season mean of a specific year (2000–2010) relative to the long-term growing season mean (\bar{x}) and standard deviation (σ) over the past decade.

The MODIS monthly composites were averaged for June, July and August (JJA) to represent the dry season mean for each year over the 2000–2010 period. Similarly, the January–February mean of MODIS LST data was used to calculate the standardized anomaly for extreme winters in the Mongolian Plateau as the maximum snow depth typically occurs in January (Morinaga *et al* 2003).

Precipitation data from the monthly TRMM 3B43 was processed similarly to provide dry season estimates of rainfall for each year over the 2000–2010 period as well as the long-term growing season mean and standard deviation. Standardized anomalies were then calculated at the pixel level for each year for both the MODIS and VIP datasets. In order to track the temporal variation, we plotted frequency histograms of the anomalies for each variable, by year and binned the data in order to quantify negative large anomalies (<–1 std.) as a percentage of vegetated area (e.g. figure 4). Positively skewed frequency distributions are characterized by negative anomalies and signify dry years, whereas negatively-skewed distributions with positive anomalies signify wet years. Finally, the EVI, PDSI and TRMM datasets were spatially averaged over the desert and grassland biomes for IM and OM independently in order to quantify and validate the interannual variability of summer and extreme winter trends at an aggregated level with a higher signal-to-noise ratio (Atkinson *et al* 2011).

The Mongolian Plateau is highly heterogeneous and can be divided into desert, grassland and forest biomes, with distinctive eco-climatic zones (figure 1, John *et al* 2009). The plateau is composed of Mongolia (former outer Mongolia, OM), and Inner Mongolia (IM) China, and they have very different trajectories of land cover/land use change

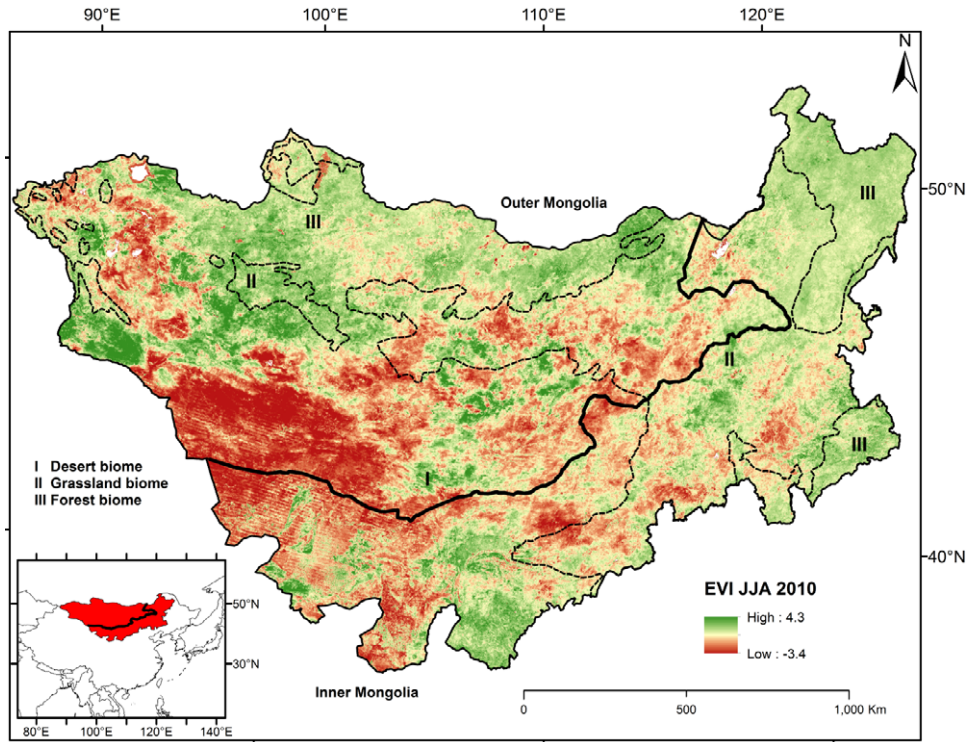


Figure 1. Standardized anomalies (summer June–July–August 2010) of MODIS-derived EVI, (MOD13A3) on the Mongolian Plateau, as compared to the decadal mean overlaid with terrestrial ecoregion (WWF) biome boundaries: desert (I), grassland (II) and forest (III).

Table 1. Proportion of vegetated area in the Mongolian Plateau covered by <-1 standardized anomalies of EVI and EVI2 during June–July–August (JJA) in summer and January–February (JF) land surface temperature anomalies in winter. Summer droughts of 2001 and 2009 and *dzud* of 2010 are highlighted in bold.

Source	Variable	Year										
		2000	2001	2002	2003	2004	2005	2006	2007	2008	2009	2010
MOD13A3	EVI JJA	2.27	8.6	0.63	0.18	0.19	2.17	1.01	0.60	1.22	5.69	1.22
VIP EVI2	EVI2JJA	3.73	14.40	2.85	0.56	1.54	4.50	2.46	4.58	1.78	4.54	0.62
MOD11A2	LST JF		50.70	28.58	48.69	44.77	72.74	45.52	29.89	56.58	39.95	69.65

(Chen *et al* 2013). This suggests that any anomaly study of vegetation productivity or land surface phenomenon should first stratify the plateau into its constituent biomes and major administrative divisions to enable the comparison of vegetation anomalies between biomes and to avoid confounding effects in interannual comparisons of anomaly trends.

We used the World Wildlife Fund (WWF) biome boundaries (Olson *et al* 2001) to stratify our study region and delineate desert, grassland and forest biomes. The desert biome in IM includes the eastern Gobi desert steppe and the Alashan Plateau semi-desert while the grassland biome primarily consists of the Mongolian–Manchurian grasslands, which extend into OM and the Ordos Plateau. The desert biome in OM includes the eastern Gobi desert steppe, Junggar basin semi-desert, Gobi lakes valley desert steppe, Great lakes basin desert steppe and Alashan Plateau desert steppe. The OM grassland biome consists mainly of the Mongolian–Manchurian grasslands but also includes the

Sayan intermontane steppe, Altai alpine meadow and the Khangai mountains alpine meadow.

3. Results

3.1. Anomalies of vegetation indices and LST at the plateau level

For both EVI and EVI2 during the eleven year period (2000–2010), areas experiencing negative anomalies were the greatest in 2001 when there was a major drought (figure 2, table 1). Thereafter, areas with negative anomalies decreased, except in 2009 when 5.6% of the area was affected (figure 2, table 1). Drought, as measured by negative TRMM rainfall anomalies and PDSI <-1 , affected a large area in 2001, including the central, southwestern and northern portions of the plateau, while the 2009 drought mainly affected the northwest, central and south eastern portions (figure 3). We found that a large proportion of the plateau ($>50%$) exhibited negative anomalies for LST in 2001, 2005, 2008 and 2010

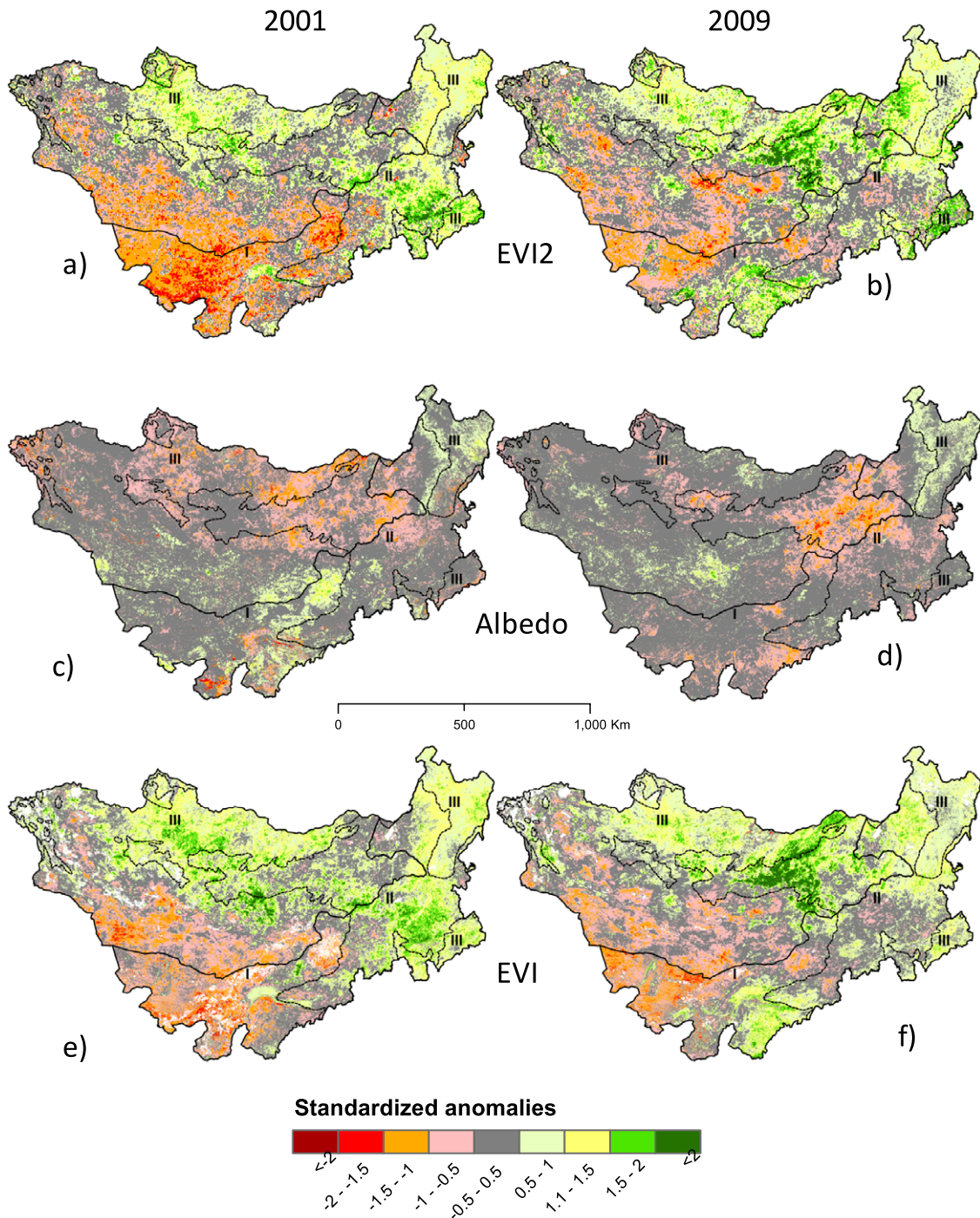


Figure 2. Standardized anomalies of EVI2, white sky albedo and EVI in 2001 ((a), (c), (e)) and 2009 ((b), (d), (f)) summer droughts (June–July–August). Negative VI anomalies ((a), (e) and (b), (f)), correlate with positive albedo anomalies ((c) and (d)) respectively.

(table 1). The *dzud* or extreme winter in 2009–2010 was tracked extremely well by JF MODIS LST with 70% of the area covered by negative anomalies while the preceding summer drought of 2009 was characterized by negative anomalies in JJA MODIS EVI and VIP EVI2 (table 1).

3.2. Anomalies of vegetation indices and LST in the desert biome

Negative anomalies of EVI and EVI2 were larger for the IM desert biome than for the OM. EVI exhibited negative

anomalies for the desert biome of IM, occupying 28.2% and 20.6% of the total vegetated area in 2001 and 2009, respectively. In comparison, only 15.1% and 10% of the vegetated area in OM exhibited negative anomalies in EVI during 2001 and 2009, respectively (figure 2, table 2). This difference between IM and OM in both years was also manifested by the longer-term VIP EVI2 dataset. MODIS LST negative anomalies in IM covered greater than 40% of the area in 2005, 2006 and 2010 and reached a maximum of 65% in 2008 (figure 2, table 2). The *dzud* extreme event of

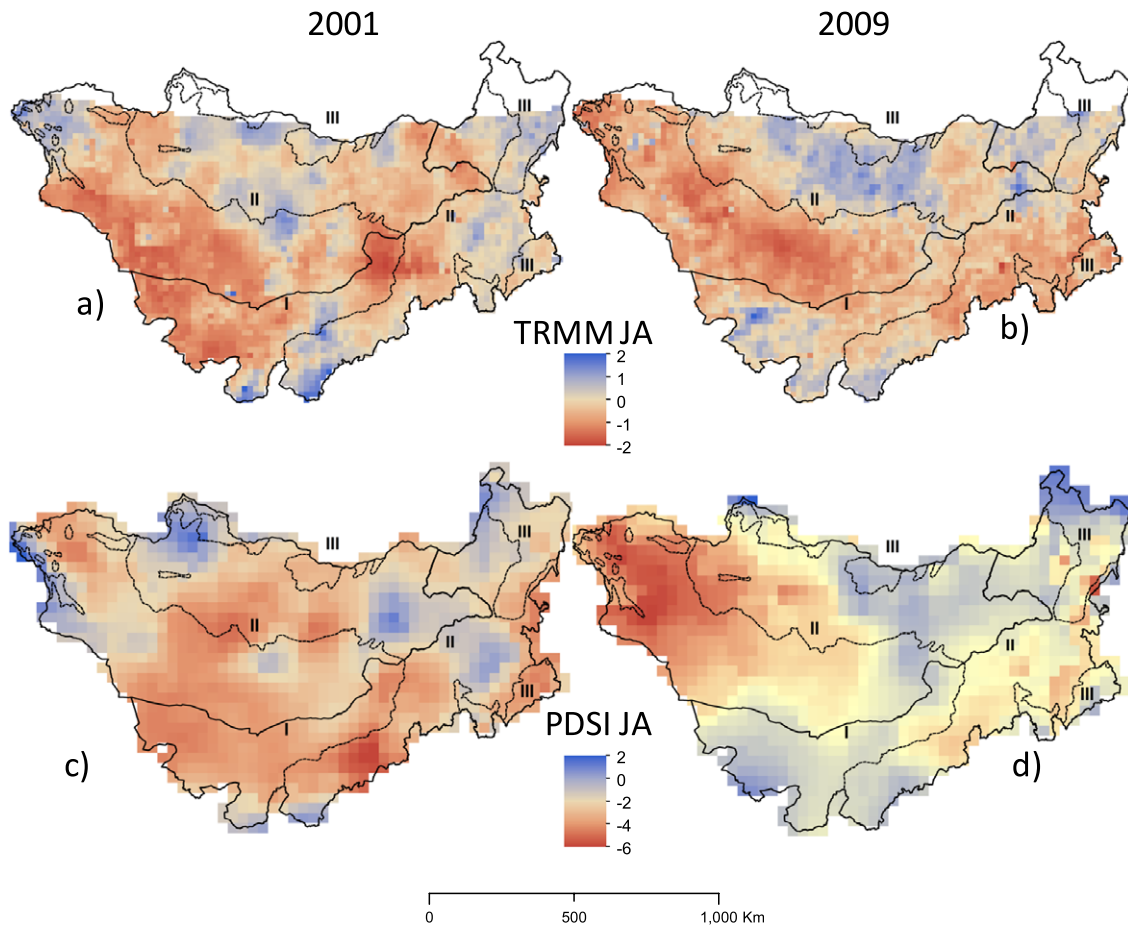


Figure 3. Standardized anomalies of June–July–August (JJA) TRMM rainfall and PDSI in 2001 ((a), (c)) and 2009 ((b), (d)) summer droughts relative to the growing season mean for 2000–2010.

Table 2. Proportion of vegetated area in the dominant desert and grassland biomes of the Mongolian Plateau covered by <math><-1</math> standardized anomalies of EVI and EVI2 during June–July–August (JJA) in summer and January–February (JF) land surface temperature anomalies in winter. Summer droughts of 2001 and 2009 and *dzud* of 2010 are highlighted in bold.

Variable	IM										OM											
	00	01	02	03	04	05	06	07	08	09	10	00	01	02	03	04	05	06	07	08	09	10
DESERT																						
EVI JJA	6.3	28.2	1.5	0.4	0.6	5.1	1.9	0.6	2.4	20.6	2.2	4.9	15.1	1.4	0	0.2	5	2.4	1	2.6	10	3.4
EVI2JJA	14.5	50.5	5.0	1.0	1.2	5.4	2.4	0.2	0.8	4.9	0.2	5.3	21.5	5.6	0.5	2.0	10.8	5.9	5.1	3.7	10.9	1.2
LST JF		20.2	14	37	24	47	45	23	65	24.5	43		31.5	35	51	33	70	27	25	49	30	62
GRASSLAND																						
EVI JJA	0.5	3.7	0.1	0.1	0.1	0.7	0.3	0.1	0.1	0.2	0.1	0	0.1	0.1	0.2	0.1	0.1	0.1	0.9	0.8	0.2	0
EVI2JJA	1.2	6.8	0.3	0.3	1.2	1.6	0.9	0.9	0.1	0.6	0.4	0.1	0.3	0.7	0.5	2.3	1.5	1.0	11	2.0	1.6	0.3
LST JF		52	17	55	48	79	59	35	52	42	69		72	29	47	52	77	42	28	60	42	83

2009–2010 was characterized by large negative anomalies of EVI/EVI2 and LST for both the IM and OM desert biome. Summer negative anomalies in 2009 preceded negative winter anomalies in MODIS LST in 2010 for both IM and OM (table 2).

MODIS EVI anomalies in the IM desert biome (figure 4(a)) in 2001 and 2009 showed a strong positive skew, characterized by negative anomalies with peak standardized anomalies of -0.75 to -1 and were significantly different

from wet years (2004 and 2007). EVI anomalies in the OM desert biome showed a positive skew in dry years (2001, 2005, 2009) and a prominently negative skew in a wet year like 2003 (figure 4(b)). Furthermore, the frequency distributions of desert biome anomalies were more evenly distributed and showed greater variation for IM (figure 4(a)) than for OM (figure 4(b)), with the notable exception of 2003 with a peak centered on $+2$ that denoted an extremely wet year. The VIP EVI2 anomalies in the desert biome were similar to the EVI

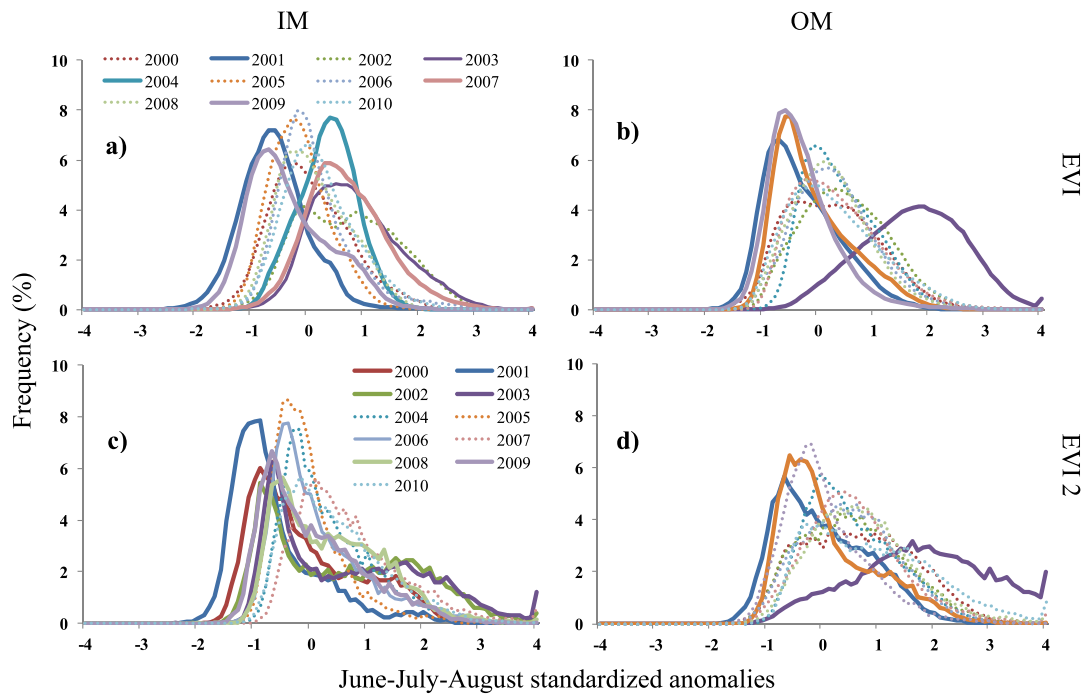


Figure 4. Frequency distributions of standardized MODIS EVI and VIP EVI2 June–July–August ((a)–(d)) anomalies in the desert biome (2000–2010) for Inner Mongolia (IM) and Outer Mongolia (OM). Positively skewed drought years (2000–2001, 2005, 2009) are characterized by the majority of negative anomalies with peak values between -1.5 and -0.5 std. and are statistically different ($p < 0.001$) from relatively wet years (2003, 2004, 2007). VIP EVI2 is based on a longer-term mean (1981–2010) than MODIS EVI.

frequency distributions with strong positive skews in 2000, 2001, 2002 and 2009 indicating negative anomalies < -1 std. in IM (figure 4(c)) and $> +1$ std. for wet years like 2003 in OM (figure 4(d)).

The extreme winter (JF) anomalies in LST for the IM desert biome showed a positive skew in 2006, 2008 and 2010 with negative anomalies reaching a peak of -1 for 2006 and 2010 and a peak of -1.5 for 2008 (supplementary figure 1(a) available at stacks.iop.org/ERL/8/035033/mmedia). The frequency distributions of LST for the IM desert biome showed greater variation than those in OM. The frequency distributions of LST for the IM desert biome exhibited slightly negative skews for relatively moderate years (2004, 2007 and 2009) (supplementary figure 1(b) available at stacks.iop.org/ERL/8/035033/mmedia).

3.3. Anomalies of vegetation indices and LST for the grassland biome

There was no significant difference between EVI and EVI2 anomalies in the IM and OM grassland biome. The proportion of area covered by negative anomalies in EVI and EVI2 was generally lower than 10% for both IM and OM (figure 2, table 2). The frequency distributions of both EVI and EVI2 anomalies were generally indicative of positive anomalies (figure 5).

The MODIS EVI anomalies for the IM and OM grassland biomes (figures 5(a)–(d)) showed strong negative skews (i.e., a majority of positive anomalies) with peak values of $+0.5$ to $+1$. The frequency distributions of EVI anomalies were tightly grouped for both the IM and OM grassland biomes

with wet years not significantly different from dry years. In comparison, the VIP EVI2 anomalies, based on a longer-term mean (1981–2010), showed greater variation and spread for the frequency distributions (figure 5). Dry years such as 2000 had peak values centered on zero for the IM grassland biome (figures 5(a) and (c)), whereas they were centered on $+0.5$ for OM grassland biome (figures 5(b) and (d)). Wet years in both IM and OM grassland biomes were centered on $+1$ (figure 5).

In IM, negative anomalies in the LST covered 50–80% of the area in 2001, 2003, 2005, 2006, 2008 and 2010. Similarly, the negative LST anomalies in OM covered 50–85% in 2001, 2004, 2005, 2008 and 2010. The *dzud* extreme winter event of 2009–2010 was more prominent for OM and IM grassland biomes than in the desert biome showing a strong positive skew in 2010, reaching a peak of -1.5 std. (supplementary figure 1(c) available at stacks.iop.org/ERL/8/035033/mmedia). In 2001, summer negative LST anomalies in IM occupying 3.7% and 6.8% in EVI and EVI2, respectively, corresponded to negative winter anomalies in January–February covering 52% of the area (table 2). Though negative LST anomalies in the winter of 2000–2001 covered 72% of OM, the preceding summer did not show evidence of anomalies from the extreme summer for the grassland biome compared to the desert biome (table 2).

3.4. Spatially averaged PDSI, TRMM and LST

The proportion of land area affected by drought (PDSI < -1) for the desert biome reached 60–80% for 2001, 2005 and 2009, showing that the desert biome was largely

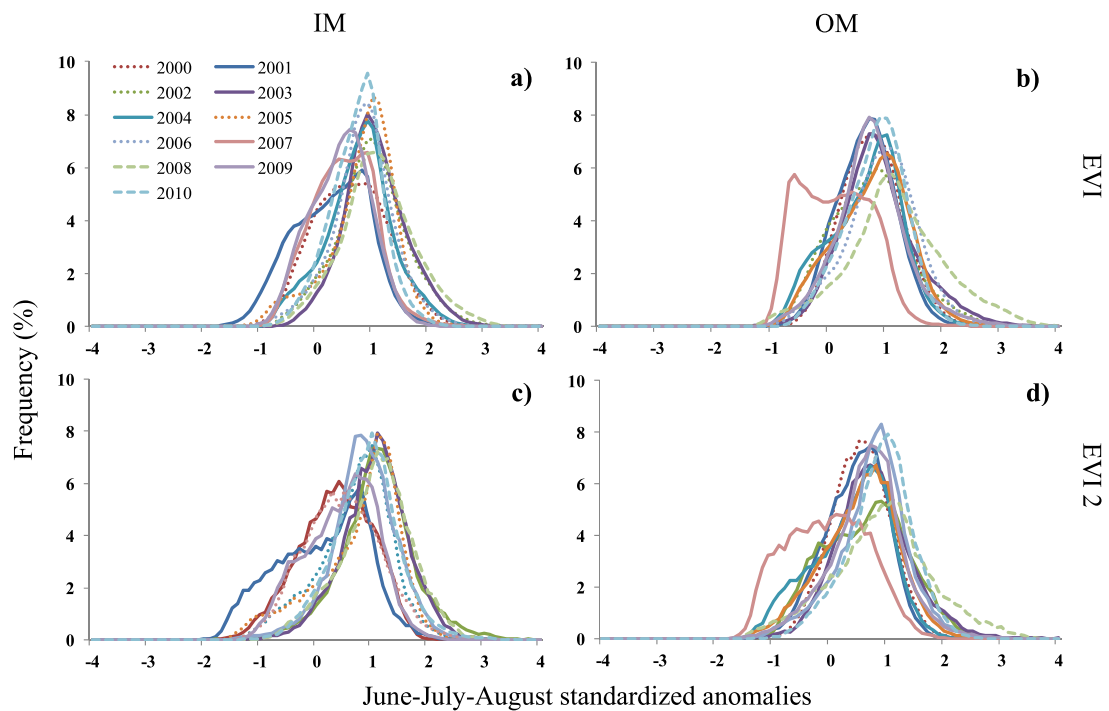


Figure 5. Frequency distributions of standardized MODIS EVI and VIP EVI2 June–July–August ((a)–(d)) anomalies in the grassland biome (2000–2010) for Inner Mongolia (IM) and Outer Mongolia (OM). The distributions of dry years are not statistically different ($p < 0.001$) from relatively wet years in the grassland biome as compared to the desert biome (note: this may suggest that the grassland ecosystems are more stable than deserts).

affected by drought for these three years (figure 3). For the 2000–2010 period the drought-affected area (%) was correlated with spatially averaged EVI for JJA (figures 6(a) and (b)) and TRMM rainfall (supplementary figures 2(a) and (b) available at stacks.iop.org/ERL/8/035033/mmedia) in both IM and OM. Even though the IM and OM grassland biomes were also largely affected by drought in 2001, 2005 and 2009, the spatially averaged EVI and TRMM values were correlated with the drought-affected area (%) for IM (figure 6(c), supplementary figure 2(c) available at stacks.iop.org/ERL/8/035033/mmedia), but not for OM (figure 6(d), supplementary figure 2(d) available at stacks.iop.org/ERL/8/035033/mmedia). A linear regression of spatially averaged EVI and proportion of PDSI < -1 for the desert biome showed strong correlations in both IM ($R^2 = 0.64, p < 0.05$) and OM ($R^2 = 0.63, p < 0.05$) (figure 6(e)). For the grassland biome, the spatially averaged EVI showed a moderately strong relationship with drought-affected areas ($R^2 = 0.41, p < 0.05$) in IM but was not significantly correlated with drought-affected areas in OM (figure 6(f)).

The spatially averaged January–February LST exhibited negative anomalies for the extreme winters of 2005, 2008 and 2010 and correlated with the proportion of area covered by LST anomalies (< -1 std.) for the IM and OM desert and grassland biomes (supplementary figure 3 available at stacks.iop.org/ERL/8/035033/mmedia). Interestingly, while there was a 20% increase in area under < -1 std. LST anomalies for the 2010 winter for the desert biome (supplementary figures 3(a) and (c)), there was corresponding 40% increase

in area for the grassland biome (supplementary figures 3(b) and (d)).

4. Discussion

4.1. Greening and extreme event trends

Northern and northwestern China have experienced changes in climate with an increase in precipitation, leading to enhanced vegetation growth in the 1980s and 1990s (Piao *et al* 2006). This is also corroborated by a decrease in PDSI < -2 over IM in the 1980s and 1990s (Dai *et al* 2004). Our analyses of EVI and EVI2 anomalies showed an increase in positive anomalies in non-drought years (e.g., 2003 and 2004; tables 1 and 2) and were consistent with previous studies (Xu *et al* 2012). A recent NDVI-based study found an increasing trend in vegetation greenness between 1982 and 2009 for the whole of China, with a corresponding increase in percentage area under positive anomalies from 27% in the late 1980s to 61% in the late 2000s (Peng *et al* 2011). This greening trend was generally consistent with earlier studies that suggested increasing greenness and primary productivity during the last two decades of the 20th century not only in China (Xiao and Moody 2004, Park and Sohn 2010, Piao *et al* 2011) but also more broadly across the middle and high latitudes of the northern hemisphere (Myneni *et al* 1997, Zhou *et al* 2001, Xiao and Moody 2005).

This greening trend, however, has been partly offset by extreme climate events such as the 2000–2002 droughts (Davi *et al* 2009, 2010). PDSI in China and the Mongolian

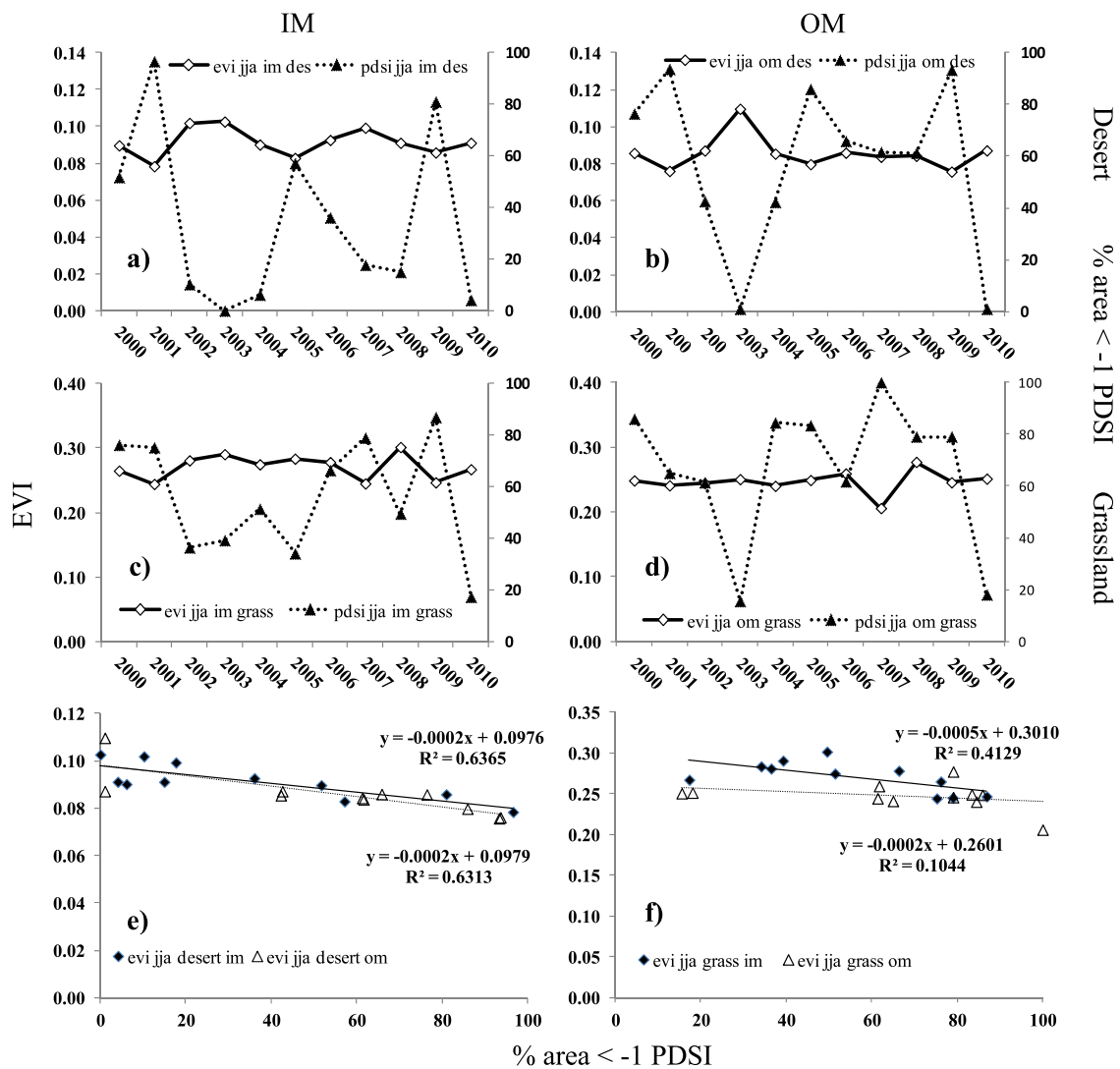


Figure 6. Area averaged means of June–July–August EVI plotted with the proportion of area covered by <-1 PDSI in desert ((a), (b)) and grassland ((c), (d)) biomes for Inner Mongolia (IM) and Outer Mongolia (OM). Linear regression of July–August EVI with the proportion of area covered by <-1 PDSI in desert (e) and grassland (f) biomes for Inner Mongolia (IM) and Outer Mongolia (OM).

Plateau showed a decreasing trend since the 1990s with 2001 being the driest year (Li *et al* 2009). Recent studies have suggested that the increasing trend in NDVI has stalled in the last decade (Park and Sohn 2010, Piao *et al* 2011, Samanta *et al* 2011). Our study showed a similar increase in per cent area under negative EVI/EVI2 anomalies in drought years (e.g., 2001 and 2009). Climate trends are complex in the study region with some studies showing increasing drought persistence in eastern Mongolia (Li *et al* 2009) while others report an increasing precipitation trend in western Mongolia (Davi *et al* 2009). These contradictory trends present a problem for studying anomalies at the scale of the entire plateau. In addition, there are two climate gradients with increasing precipitation and a decrease in temperature from the southwest to northeast in IM and from the south to north in OM. Our analysis stratified the anomalies by the two dominant biome types as well as by political boundaries owing to divergent land cover/land use trajectories (Chen *et al* 2013).

4.2. Vulnerability and resilience of desert and grassland biomes

We found that the desert biomes were slightly more vulnerable and less resilient to drought than the grassland biome on the plateau. Sui *et al* (2013) showed that while the desert steppe had a lower carbon sink capacity than a typical/meadow steppe, it had the highest standard deviation (108 g cm^{-2}). Teuling *et al* (2010) suggested that grasslands were less resilient than forests during heat wave events in which high temperature and evapotranspiration led to soil moisture depletion and further suppressed plant productivity. This is probably only true of short-term droughts, as other studies suggested a quick recovery in grasslands following summer droughts in the past decade (Xu *et al* 2012, Ponce-Campos *et al* 2013).

The meadow steppe within the grassland biome had low interannual variability in annual precipitation with coefficient of variation (CV) less than 0.21 (Yu *et al* 2003); in comparison, the desert biome exhibited higher interannual

variability in annual precipitation ($CV > 0.40$) (Ellis 1992). Bai *et al* (2004) suggested that ecosystem stability as measured by the CV of aboveground biomass increased from the species to plant functional group and to the community level for IM grasslands with precipitation from January to July explaining up to 49% of the variation. We argue that some herbaceous desert steppe species were less resilient than species of typical and meadow steppes within the grassland biome owing to greater per cent cover and precipitation (John *et al* 2008). Cheng *et al* (2007) suggests that dominant herbaceous grass species like *Stipa bungeana* were being replaced by xerophyte shrubs like *Artemisia ordosica* and *Cynachum komarovi* on the Ordos Plateau—one of the ecoregions within the desert biome. *Stipa* and *Cynachum* spp. had shallow roots and depended on light rain events, while *Artemisia* spp. had deeper roots and depended on larger rain events (Cheng *et al* 2007).

4.3. Ecological implications of drought and dzud

Few studies have used satellite data to help characterize extreme winters which are a major climate phenomenon unique to the plateau. For example, Tachiiri *et al* (2008) used a snow water equivalent to measure snow cover in conjunction with summer NDVI in order to predict livestock mortality. We used the percentage of land area covered by negative LST anomalies to characterize the extreme winter *dzud* events in 2001 and 2010. Since *dzud* events are often influenced by the previous summer (Tachiiri *et al* 2008), we found that negative EVI/EVI2 summer anomalies in 2009 preceded negative LST anomalies (> -1 std.) in January–February 2010.

Semiarid ecosystems like the desert steppe on the Mongolian Plateau (>150 mm annual rainfall) are driven by low precipitation with high variability to operate in a non-equilibrium manner, i.e., abiotic control on plant biomass (Sullivan 1996). Here, the influence of abiotic factors like precipitation variability is more important than density-dependent feedback from grazing herds (Fernández-Giménez and Allen-Diaz 1999). In comparison, the meadow-mountain (350–400 mm annual precipitation) steppe conforms to the more conventional range control model of grazing density dynamics where increased grazing leads to a decrease in grass species and an increase in forbs and annual weeds (Fernández-Giménez and Allen-Diaz 1999). The typical steppe (200–300 mm annual precipitation) lies between the desert steppe and meadow steppe. Grass and other vegetation cover in the typical steppe respond interactively in an intermediate fashion to a combination of annual precipitation dynamics and grazing pressure, with changes similar to the range control model in species composition (Fernández-Giménez and Allen-Diaz 1999).

The Mongolian Plateau received above average rainfall in the mid-1990s that led to an increase in livestock numbers (Retzer and Reudbach 2005). This increased grazing pressure was compounded by socio-economic changes following the collapse of collectivization. These changes included decreased migration, fewer functioning wells (previously maintained by the government) and private ownership of

livestock by sedentary herders (Sternberg 2008). In this context, Retzer and Reudbach (2005) suggested that the uncontrolled increase in livestock, in numbers more suited for equilibrium conditions (grazing density control), could not be sustained in a non-equilibrium system (with abiotic factor control) and led to high livestock mortality. Reduced grazing pressures following a combined summer drought–*dzud* event will have positive ecological feedback in terms of increased grass biomass and canopy cover relative to forbs, shrubs and weedy annuals.

4.4. Anomalies explained by land cover/use changes

Some of the positive anomalies in drought and non-drought years (e.g., in north-central OM) could be explained by the recent increase in cropland area following the major, persistent drought of 2000–2002 (Regdel *et al* 2012). Mongolia initiated a program called *Atar 3*, aka, the ‘Third Campaign to Reclaim Abandoned Agriculture Lands’, which increased government spending between 2005 and 2009 in order to improve food security and prevent future food crises (Pederson *et al* 2013). Most of the increase in cropland cover is in the Bulgan, Selenge and Tov *aimags* (first-level administrative subdivision) around the capital, Ulaanbaatar (Pederson *et al* 2013). A similar increase in agricultural cover could also partly explain the increase in positive anomalies during drought and non-drought years in IM (figure 2). However, there was a reduction of cropland cover in some regions of IM during the same period. Wang *et al* (2012) suggested that northwestern China experienced a decrease in croplands during 1996–2000 when IM lost 3.3×10^4 ha due to the ‘*Grain for Green*’ program. The policy was designed to shift 15 million hectares of low-yield cropland to forest as well as the afforestation of barren hillsides by offering grain and cash to farmers as compensation for land conversion (Feng *et al* 2005, Long *et al* 2006).

EVI/EVI2 anomalies were inversely related to white sky albedo anomalies during the summer droughts of 2001 and 2009. Negative anomalies (< -1) in EVI/EVI2 for both desert and grassland biomes corresponded to positive albedo anomalies (> 1) (figure 2). These positive albedo anomalies, indicative of reduced per cent cover, occurred along the typical steppe–desert steppe interface in the grassland–desert ecotone. Conversely, positive VI anomalies (> 1) for both desert and grassland biomes corresponded to negative albedo anomalies (< -1), which could be explained in part by irrigated agriculture in IM and cropland expansion in north-central OM. This suggested that the vegetation anomalies were not false signals caused by clouds and/or aerosol-contaminated pixels.

5. Conclusions

The 2000–2002 combined summer drought–*dzud* and 2009–2010 *dzud* were severe and affected most of the Mongolian Plateau. This region has seen an increased frequency of extreme climatic events in the last decade as compared to the previous 20 years. We assessed the extent and

severity of drought and extreme winters using precipitation and PDSI data and examined the vegetation response to these extreme events using anomalies of vegetation indices and LST derived from MODIS and AVHRR. We found significant differences in biome response which was unique in both the decadal (MODIS) and multi-decadal (AVHRR) satellite-based greenness records. Our results showed that the grassland biome on the plateau was more resilient to drought than the desert biome. Finally, the longer-term EVI2 record validated our 11-year MODIS EVI record showing that there was a differential response in the desert and grassland biome and that it was observed at both time scales (deviations from an 11-year and 30-year mean). There is a need for further investigation of vegetation response due to possible ecological as well as socio-economic impacts such as grazing, urban expansion and increase in cropland cover. A reduction in grazing pressure following extreme climatic events such as *dzud* might have positive feedback in terms of increased grass biomass and canopy cover as compared to shrubs and weedy annuals.

Acknowledgments

This study was supported by the NASA-NEWS Program (NN-H-04-705 Z-YS-005-N), the Natural Science Foundation of China (31229001), the Outstanding Overseas Scientists Team Project of the Chinese Academy of Sciences and the State Key Basic Research Development Program of China (2007CB106800). J Xiao was partly supported by the National Science Foundation (NSF) through MacroSystems Biology (award number 1065777) and NASA through the Carbon Monitoring System (NNX11AL32G). We would like to thank Lisa Delp Taylor and Dee Becker who proofread the manuscript at various stages, Mohamed Abd salam El Vilaly and Kirk Zmijewski for RS data processing suggestions and Kamel Didan for kindly providing travel support to the VIP data workshop at the University of Arizona in January 2013.

References

- Aizen E, Aizen V, Melack J, Nakamura T and Ohta T 2001 Precipitation and atmospheric circulation patterns at mid latitudes of Asia *Int. J. Climatol.* **21** 535–56
- Anderson L O, Malhi Y, Aragao L, Ladle R, Arai E, Barbier N and Phillips O 2010 Remote sensing detection of droughts in Amazonian forest canopies *New Phytol.* **187** 733–50
- Angerer J, Guodong H, Fujisaki I and Havstad K 2008 Climate change and ecosystems of Asia with emphasis on Inner Mongolia and Mongolia *Rangelands* **30** 46–51
- Aragao L, Malhi Y, Roman Cuesta R M, Saatchi S, Anderson L O and Shimabukuro Y E 2007 Spatial patterns and fire response of recent Amazonian droughts *Geophys. Res. Lett.* **34** L07701
- Atkinson P M, Dash J and Jegathanan C 2011 Amazon vegetation greenness as measured by satellite sensors over the last decade *Geophys. Res. Lett.* **38** L19105
- Bai Y, Han X, Wu J, Chen Z and Li L 2004 Ecosystem stability and compensatory effects in the Inner Mongolia grassland *Nature* **431** 181–4
- Brando P M, Goetz S J, Baccini A, Nepstad D C, Beck P S A and Christman M C 2010 Seasonal and interannual variability of climate and vegetation indices across the Amazon *Proc. Natl Acad. Sci.* **107** 14685–90
- Chen J et al 2013 State and change of Dryland East Asia (DEA) *Dryland East Asia (DEA): Land Dynamics Amid Social and Climate Change* ed J Chen, S Wan, G Henebry, J Qi, G Gutman, G Sun and M Kappas (Berlin: HEP and De Gruyter) at press
- Cheng X, An S, Chen J, Li B, Liu Y and Liu S 2007 Spatial relationships among species, above-ground biomass, N and P in degraded grasslands in Ordos Plateau, northwestern China *J. Arid Environ.* **68** 68–7
- Dai A, Trenberth K E and Qian T 2004 A global data set of Palmer drought severity index for 1870–2002: relationship with soil moisture and effects of surface warming *J. Hydrometeorol.* **5** 1117–30
- Davi N, Jacoby G, D'Arrigo R, Baatarbileg N, Li J and Curtis A A 2009 Tree-ring based drought index reconstruction for Far Western Mongolia: 1565–2004 *Int. J. Climatol.* **29** 1508–14
- Davi N, Jacoby G, Fang K, Li J, D'Arrigo R, Baatarbileg N and Robinson D 2010 Reconstructed drought across Mongolia based on a large-scale tree-ring network: 1520–1993 *J. Geophys. Res. D* **15** D22103
- Donohue R J, McVicar T R and Roderick M L 2009 Climate-related trends in Australian vegetation cover as inferred from satellite observations, 1981–2006 *Glob. Change Biol.* **15** 1025–39
- Ellis J 1992 Key issues in grassland studies *Grasslands and Grassland Sciences in Northern China* ed J Ellis (Washington, DC: National Academies Press) pp 183–98
- Feng Z, Yang Y, Zhang Y, Zhang P and Li Y 2005 Grain-for-green policy and its impacts on grain supply in West China *Land Use Policy* **22** 301–12
- Fernández-Giménez M E and Allen-Diaz B 1999 Testing a nonequilibrium model of rangeland vegetation dynamics in Mongolia *J. Appl. Ecol.* **36** 871–85
- Fernández-Giménez M E, Batkhishig B and Batbuyan B 2012 Cross-boundary and cross-level dynamics increase vulnerability to severe winter disasters (*dzud*) in Mongolia *Glob. Environ. Change* **22** 836–51
- Groisman P Y et al 2009 The northern Eurasia earth science partnership: an example of science applied to societal needs *Bull. Am. Meteorol. Soc.* **90** 671–88
- Hansen J, Ruedy R, Sato M and Lo K 2010 Global surface temperature change *Rev. Geophys.* **48** RG4004
- Huete A, Didan K, Miura T, Rodriguez E, Gao X and Ferreira L G 2002 Overview of the radiometric and biophysical performance of the MODIS vegetation indices *Remote Sens. Environ.* **83** 195–213
- Huete A R, Didan K, Shimabukuro Y E, Ratana P, Saleska S R, Hutyrá L R, Yang W, Nemani R and Myneni R 2006 Amazon rainforests green up with sunlight in dry season *Geophys. Res. Lett.* **33** L06405
- Huffman G, Adler R, Rudolf B, Schneider U and Keen P 1995 Global precipitation estimates based on a technique for combining satellite based estimates, rain gauge analysis, and NWP model precipitation information *J. Clim.* **8** 1284–95
- Iwao K and Takahashi M 2006 Interannual change in summertime precipitation over northeast Asia *Geophys. Res. Lett.* **33** L16703
- Jiang Z Y, Huete A R, Didan K and Miura T 2008 Development of a two-band enhanced vegetation index without a blue band *Remote Sens. Environ.* **112** 3833–45
- John R, Chen J, Lu N, Guo K, Liang C, Wei Y, Noormets A, Ma K and Han X 2008 Predicting plant diversity based on remote sensing products in the semi-arid region of Inner Mongolia *Remote Sens. Environ.* **112** 2018–32
- John R, Chen J, Lu N and Wilske B 2009 Land cover/land use change in semi-arid Inner Mongolia: 1992–2004 *Environ. Res. Lett.* **4** 045010
- Lewis S L, Brando P M, Phillips O L, van der Heijden G M F and Nepstad D 2011 The 2010 Amazon drought *Science* **331** 554

- Li J, Cook E, D'Arrigo R, Chen F and Gou X 2009 Moisture variability across China and Mongolia *Clim. Dyn.* **32** 1173–86
- Long H L, Heilig G K, Wang J, Li X B, Luo M, Wu X Q and Zhang M 2006 *Land Degrad. Dev.* **17** 589–603
- Lu N, Wilske B, Ni J, John R and Chen J 2009 Climate change in Inner Mongolia from 1955–2005—trends at regional, biome and local scales *Environ. Res. Lett.* **4** 045006
- Morinaga Y, Tian S F and Shinoda M 2003 Winter snow anomaly and atmospheric circulation in Mongolia *Int. J. Climatol.* **23** 1627–36
- Myneni R B, Deeling C D, Tucker C J, Asrar G and Nemani R R 1997 Increased plant growth in the northern high latitudes from 1981 to 1991 *Nature* **386** 698–702
- Myneni R B, Hall F G, Sellers P J and Marshak A L 1995 The interpretation of spectral vegetation indexes *IEEE Trans. Geosci. Remote Sens.* **33** 481–6
- New M, Hulme M and Jones P 2000 Representing twentieth-century space–time climate variability. Part II: development of a 1961–90 mean monthly terrestrial climatology *J. Climatol.* **13** 2217–38
- Olson D M *et al* 2001 Terrestrial ecoregions of the world: a new map of life on earth *Bioscience* **51** 933–8
- Palmer W C 1965 *Meteorological Drought Research Paper No. 45* (Washington, DC: US Department of Commerce) p 58
- Park H S and Sohn B J 2010 Recent trends in changes of vegetation over East Asia coupled with temperature and rainfall variations *J. Geophys. Res. D* **115** D14101
- Pederson N, Leland C, Nachin B, Hessel A E, Bell A R, Martin-Bennito D, Saladyga T, Suran B, Brown P M and Davi N 2013 Three centuries of shifting hydroclimatic regimes across the Mongolian Breadbasket *Agric. Forest Meteorol.* **178–179** 10–20
- Peng S S, Chen A P, Xu L, Cao C X, Fang J Y, Myneni R B, Pinzon J E, Tucker C J and Piao S L 2011 Recent change of vegetation growth trend in China *Environ. Res. Lett.* **6** 044027
- Philips O L *et al* 2009 Drought sensitivity of the Amazon rainforest *Science* **323** 1344
- Piao S, Mohammat A, Fang J, Cai Q and Feng J 2006 NDVI-based increase in growth of temperate grasslands and its responses to climate changes in China *Glob. Environ. Change* **16** 340–8
- Piao S L, Wang X H, Ciais P, Zhu B, Wang T and Liu J 2011 Changes in satellite-derived vegetation growth trend in temperate boreal Eurasia from 1982 to 2006 *Glob. Change Biol.* **17** 3228–39
- Ponce-Campos G E *et al* 2013 Ecosystem resilience despite large-scale altered hydroclimatic conditions *Nature* **494** 349–52
- Qi J, Chen J, Wan S and Ai L 2012 Understanding the coupled natural and human systems in Dryland East Asia *Environ. Res. Lett.* **7** 015202
- Regdel D, Dugarzhav C and Gunin P D 2012 Ecological demands on socioeconomic development of Mongolia under climate aridization *Arid Ecosyst.* **2** 1–10
- Retzer V and Reudbach C 2005 Modelling the carrying capacity and coexistence of pika and livestock in the mountain steppe of the South Gobi, Mongolia *Ecol. Modelling* **189** 89–104
- Reynolds J F *et al* 2007 Global desertification: building a science for dryland development *Science* **316** 847–51
- Samanta A, Costa M H, Nunes E L, Vieira S A, Xu L and Myneni R M 2011 Comment on 'Drought-induced reduction in global terrestrial net primary production from 2000 through 2009' *Science* **333** 1093c
- Samanta A, Ganguly S, Hashimoto H, Devadiga S, Vermote E, Knyazikhin Y, Nemani R R and Myneni R B 2010 Amazon forests did not green up during the 2005 drought *Geophys. Res. Lett.* **37** L05401
- Samanta A, Ganguly S, Vermote E, Nemani R R and Myneni R B 2012 Interpretation of variations in MODIS-measured greenness levels of Amazon forests during 2000–2009 *Environ. Res. Lett.* **7** 024018
- Schwalm C R, Williams C A, Schaefer K, Baldocchi D, Black A, Goldstein A H, Law B E, Oechel W C, Paw U K T and Scott R L 2012 Reduction in carbon uptake during turn of the century drought in western North America *Nature Geosci.* **5** 551–6
- Snyder P K, Delire C and Foley J A 2004 Evaluating the influence of different vegetation biomes on the global climate *Clim. Dyn.* **23** 279–302
- Sternberg T 2008 Environmental challenges in Mongolia's dryland pastoral landscape *J. Arid Environ.* **72** 1294–304
- Sui X, Zhou G and Zhuang Q 2013 Sensitivity of carbon budget to historical climate variability and atmospheric CO₂ concentration in temperate grassland ecosystems in China *Clim. Change* **117** 259–72
- Sullivan S 1996 Towards a non-equilibrium ecology: perspectives from an arid land *J. Biogeogr.* **23** 1–5
- Tachiiri K, Shinoda M, Klinkenberg B and Morinaga Y 2008 Assessing Mongolian snow disaster risk using livestock and satellite data *J. Arid Environ.* **72** 2251–63
- Teuling A J *et al* 2010 Contrasting response of European forest and grassland energy exchange to heatwaves *Nature Geosci.* **3** 722–7
- Wang J, Chen Y, Shao X, Zhang Y and Cao Y 2012 Land-use changes and policy dimension driving forces in China: present, trend and future *Land Use Policy* **29** 737–49
- Xiao J and Moody A 2004 Trends in vegetation activity and their climatic correlates: China 1982–1998 *Int. J. Remote Sens.* **25** 5669–89
- Xiao J and Moody A 2005 Geographic distribution of global greening trends and their climatic correlates: 1982–1998 *Int. J. Remote Sens.* **26** 2371–90
- Xu L, Samanta A, Costa M H, Ganguly S, Nemani R R and Myneni R B 2011 Widespread decline in greenness of Amazonian vegetation due to the 2010 drought *Geophys. Res. Lett.* **38** L07402
- Xu X, Piao S, Wang X, Chen A, Ciais P and Myneni R M 2012 Spatio-temporal patterns of the area experiencing negative vegetation growth anomalies in China over the last three decades *Environ. Res. Lett.* **7** 035701
- Yi C *et al* 2010 Climate control of terrestrial carbon exchange across biomes and continents *Environ. Res. Lett.* **5** 034007
- Yu F F, Price K P, Ellis J and Shi P 2003 Response of seasonal vegetation development to climatic variations in eastern central Asia *Remote Sens. Environ.* **87** 42–54
- Zhang L, Xiao J, Li J, Wang K, Lei L and Guo H 2012 The 2010 spring drought reduced primary productivity in southwestern China *Environ. Res. Lett.* **7** 045706
- Zhao M and Running S W 2010 Drought-induced reduction in global terrestrial net primary production from 2000 through 2009 *Science* **329** 940–3
- Zhou L M, Tucker C J, Kaufmann R K, Slayback D, Shabanov N V and Myneni R B 2001 Variations in northern vegetation activity inferred from satellite data of vegetation index during 1981–1999 *J. Geophys. Res. D* **106** 20069–83